SciEn

Proceedings of 8th International Conference on Mechanical Engineering and Renewable Energy 2025
10-12 December, 2025, Chattogram, BANGLADESH

SciEn Conference Series: Engineering Vol. 4, 2026, pp 35-40 https://doi.org/10.38032/scse.2026.4.24

Enhanced Thermal Performance of Shell-And-Tube Heat Exchangers Using Fe_3O_4 and Al_2O_3 Nanofluids: A CFD-Based Comparative Study

Asaduzzaman Sakib[1], Usama Ibn Aziz[2], Md. Samin Khan Hridoy[3], Fahim Tanvir[4], Swagoto Ray[5]
Mohammad Nahidul Islam[*,6]

[1,4]Department of Energy Science & Engineering, Khulna University of Engineering & Technology, Khulna-9203, Bangladesh
[2]Department of Mathematics, University of Chittagong, Chattogram-4331, Bangladesh
[3,5,6]Department of Chemical Engineering, Khulna University of Engineering & Technology, Khulna-9203, Bangladesh

ABSTRACT

Shell-and-tube heat exchangers (STHEs) are widely used but limited by the low thermal conductivity of conventional fluids. This study uses CFD simulations to compare the thermal performance of Fe_3O_4-water and Al_2O_3-water nanofluids in an STHE under laminar flow. Nanoparticle concentrations of 5–20% and Reynolds numbers of 200-1000 were tested. Model validation showed deviations within ±8%. Results reveal that both nanofluids enhance heat transfer, with Fe_3O_4 consistently outperforming Al_2O_3. At ϕ = 20% and Re = 1000, Fe_3O_4 achieved a maximum heat transfer coefficient of 306.95 W/m²·K, about 318% higher than water and 40% above Al_2O_3. Temperature contours confirmed thinner boundary layers and greater heat removal for Fe_3O_4, highlighting its superior thermal capability for compact heat exchanger applications.

Keywords: Shell-and-tube heat exchanger, Nanofluid, Fe_3O_4, Al_2O_3, CFD

1. Introduction

The role of heat exchangers within thermal systems is crucial in terms of facilitating effective transfer of heat between hot and cold fluids in a broad spectrum of industrial uses such as power generation, refrigeration, chemical processing, petrochemical refining and thermal management of vehicles. The energy efficiency, fuel consumption, and operational costs of heat exchangers are directly dependent on the performance of the heat exchanger, thus its optimization has become a worldwide concern in terms of energy conservation and decarbonization [1], [2].

The most commonly used design is the shell-and-tube heat exchanger (STHE) because of its mechanical strength, modularity, and flexibility to extreme pressure and temperature operating environments [3]. Nevertheless, in spite of decades of design optimization, the overall performance of STHEs is still restrained by poor thermal conductivity of conventional working fluids including water, ethylene glycol and mineral oils [4]. These fluids have thermal conductivity values of between 0.6 and 0.7 W/mK, limiting the convective heat transfer coefficient and, thus, compactness and efficiency of exchangers.

To address these drawbacks, scientists have explored nanofluids that are man-made colloidal suspensions of nanoparticles of metallic or oxide suspended in the base fluids [5]. Nanofluids have an increased thermal conductivity, altered viscosity, and an improved convective transport property over their underlying fluids [6]. Aluminum oxide (Al_2O_3) and iron oxide (Fe_3O_4) nanoparticles have drawn the attention of many candidates among others. Al_2O_3 nanoparticles gain much attention because of a high stability, low cost and heat transfer enhancement at low concentrations [7], [8]. Instead, Fe_3O_4 nanoparticles can not only be more thermally conductive (80.4 W/mK vs. 40 W/mK in Al_2O_3) [7], but also magnetic responsive, to allow other uses in magnetically controlled thermal systems [9].

Nanofluids have potential in heat exchangers, which is proved by experimental studies. Peyghambarzadeh et al. [5] have shown that Al_2O_3-water nanofluids have the potential of enhancing heat transfer by over 20 percent at low particle concentration (less than 1 percent). According to Najim et al. [9], Fe_3O_4-water nanofluids enhanced the performance of STHEs by a maximum of 25 percent.

In spite of these developments, there are a number of gaps in the literature. To begin with, the majority of studies have been limited to low nanoparticle concentrations (less than 5 percent), which is largely explained by the fact that high nanoparticle concentrations may cause higher viscosity and penalties in pumping. Second, there are no direct comparative studies of Al_2O_3 and Fe_3O_4 nanofluids under the same flow and geometrical conditions. Third, most of the past literature has been devoted to experimental settings, which, although desirable, can be expensive and limited in scope.

This research paper aims at filling in these gaps by conducting a comparative CFD based analysis of the thermal performance of STHE using Fe_3O_4-water and Al_2O_3-water nanofluids with a concentration of 5, 10, and 20 percent and Reynolds numbers of 200, 600, and 1000 during laminar flows. Besides the overall heat transfer performance comparison, the paper also gives an in-depth discussion of

*Corresponding Author Email Address: nahidulislam.che@gmail.com

the temperature distributions, trends in the aspect of Nusselt number, and its validation with the existing correlations and experimental data. The originality of the authors is that the work focuses on a high concentration of nanoparticles, a direct comparison of the Fe_3O_4 vs. Al_2O_3, and comprehensive CFD-based findings that close the gaps that exist in literature.

2. Methodology

2.1 **Physical Domain and Geometry**

A three-dimensional STHE model was developed, consisting of 16 straight tubes arranged in-line within a cylindrical shell, with four baffles installed to enhance shell-side turbulence. Nanofluid flows through the tube side while water circulates in the shell side.

Heat exchanger parameters:

- Shell diameter: 520mm
- Tube diameter: 40mm
- Number of baffles: 4
- Baffle cut: *25%*
- Wall material: Copper

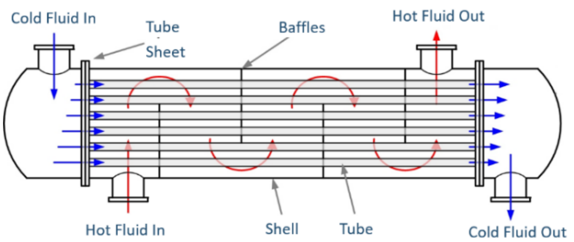

(Fig. 1 shows the modeled geometry.)

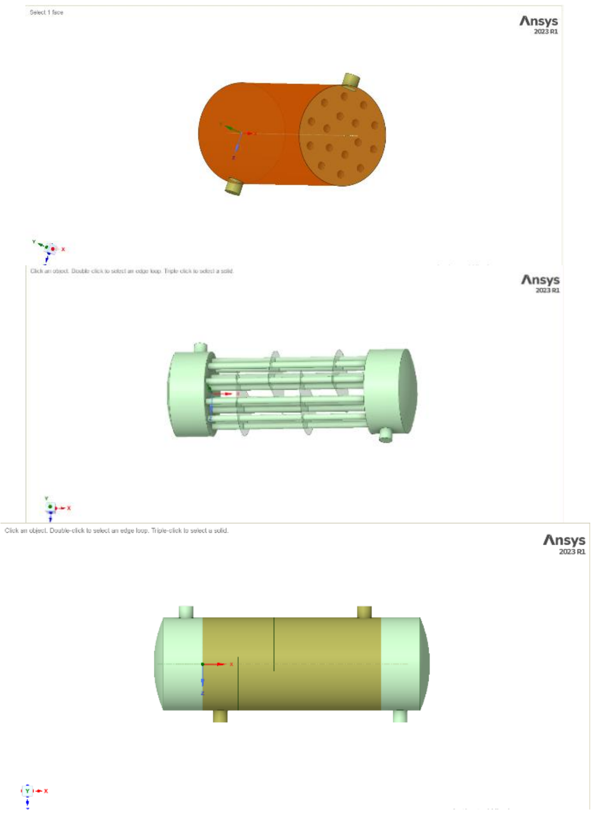

Fig. 1: Schematic diagram of the shell-and-tube heat exchanger, Geometry – water domain, nanofluid domain and full geometry

2.2 **Meshing Configuration**

The shell-and-tube heat exchanger was meshed in ANSYS Fluent with the poly-hexcore method which was a good compromise between accuracy and efficiency. Mesh sizes were 0.00151 m to 0.02414 m, relying on a 1.2 growth rate and curvature-based refinement, and produced 2400K cells and 2.4 million nodes. The refinement around the tubes and baffles was able to capture the sharp thermal and flow gradients, and the poly-hexcore geometry can offer structural layers in the wall, polyhedral core, and be stable with less number of cells during the simulation.

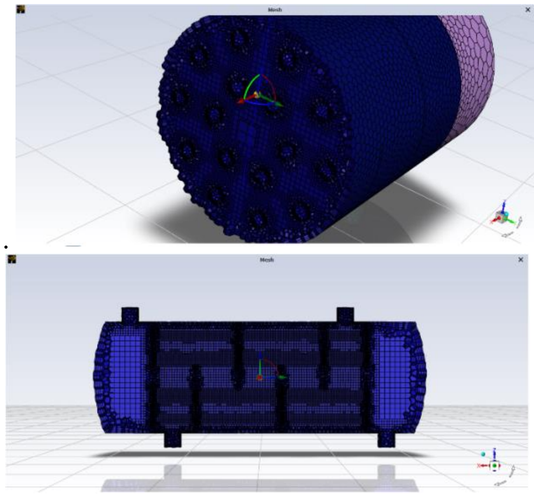

Figure 2: Mesh

A grid independence study was conducted to verify that the numerical predictions are independent of mesh resolution. Four levels of grid refinement, namely *Coarser*, *Coarse*, *Fine*, and *Finer*, were tested for Fe_3O_4 - water and Al_2O_3-water nanofluids at three Reynolds numbers (Re=200,600,1000). The average Nusselt number (Nu) was used as the evaluation parameter, and the results are summarized in “Table 1a” and “Table 1b”.

As shown, the predicted Nu values increase with mesh refinement for both nanofluids. However, the difference between the *Fine* and *Finer* grids is less than 4% at all Reynolds numbers, confirming that further mesh refinement has only a marginal effect on the results. Therefore, the *Fine* grid was selected for subsequent simulations, as it ensures sufficient numerical accuracy while maintaining computational efficiency.

Table 1(a). Grid independence test for Fe_3O_4–water nanofluid (Nu)

Grid	**Re=200**	**Re=600**	**Re=1000**
Coarser	96.693	173.041	260.907
Coarse	105.793	189.328	285.464
Fine	113.756	203.578	306.950
Finer	118.306	211.721	319.228

Table 1(b). Grid independence test for Al_2O_3-water nanofluid (Nu)

Grid	**Re=200**	**Re=600**	**Re=1000**
Coarser	87.194	153.389	186.470
Coarse	95.400	167.826	204.020
Fine	102.581	180.458	219.376
Finer	106.684	187.676	228.151

2.3 **Thermophysical Properties**

The shell-and-tube heat exchanger. To determine the heat, the thermophysical properties of water, Fe_3O_4, and Al_2O_3 used in the present study are summarized in "**Table 2**". These values were sourced from established experimental datasets in the literature and represent standard reference conditions.

Table 2. Thermophysical properties of base fluid and nanoparticles

Medium	C_p (J/kg·K)	μ (Pa·s)	k (W/m·K)	ρ (kg/m)
Water	4182	0.001	0.6	998.2
Fe_3O_4	670	–	80.4	5180
Al_2O_3	765	–	40	3970

The effective thermophysical properties of nanofluids were calculated using standard mixture models [2], [4]:

Viscosity:

$$\mu_{nf} = \mu_{bf}(1 + 2.5\varphi) \tag{1}$$

Density:

$$\rho_{nf} = (1 - \varphi)\rho_f + \varphi_p \tag{2}$$

Thermal conductivity (Maxwell model):

$$k_{nf} = \frac{k_p + 2k_f + 2(k_p - k_f)\varphi}{k_p + 2k_f - 2(k_p - k_f)\varphi} k_f \tag{3}$$

Specific heat capacity:

$$Cp_{nf} = \frac{(1-\varphi)(\rho C_p)_f + (\rho C_p)_p}{(1-\varphi)\rho_f + \varphi\rho_p} k_f \tag{4}$$

Here, ϕ is the nanoparticle volume fraction, subscripts *nf*, *bf*, *f*, and *p* denote nanofluid, base fluid, fluid, and particle respectively.

2.4 Boundary Conditions

- **Shell side:** Cold water inlet at 0.5 kg/s, 290 K; pressure outlet at 0 Pa.
- **Tube side:** Nanofluid inlet velocity adjusted for target Reynolds number, inlet temperature 388 K; outlet at 0 Pa.
- All walls were stationary, no-slip, and thermally coupled. Outer surfaces were insulated.

2.4 Boundary Conditions

To verify the accuracy of the CFD model, the simulated Nusselt numbers were compared against well-established empirical correlations, including those of Shah–London and Sieder–Tate, as well as recent experimental data from the literature. Results were benchmarked against the Fe_3O_4–water nanofluid experimental study reported by [9] in which convective heat transfer in laminar and transitional regimes was characterized. As shown in "Fig. 3", the present numerical results closely follow both classical correlations and the experimental data, with deviations generally within ±8 % across the tested Reynolds number range. Agreement with [9] was particularly strong at higher Reynolds numbers, confirming that the CFD framework can reliably capture nanoparticle-induced heat transfer enhancement mechanisms in STHEs. The ~8% deviation arises mainly from the use of semi-empirical nanofluid property correlations, simplifications in turbulence modeling, and uncertainties in the reference experimental data. Such variation is within the ±10% range commonly reported in CFD-experimental comparisons, confirming the reliability of the present model for further analysis.

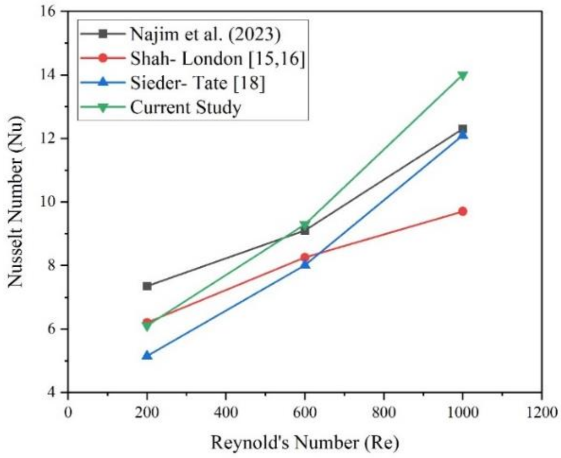

Fig. 3: Validation of current work with literature correlations and experimental data

3. Results And Discussion

3.1 Effect Of Nanoparticle Concentration

The variation of convective heat transfer coefficient (h) with nanoparticle volume fraction is shown in "Fig. 3" for Al_2O_3–water and Fe_3O_4–water nanofluids at different Reynolds numbers. In both cases, h increases monotonically with ϕ due to the enhancement in thermal conductivity (Eq. 4) and intensified micro-convection induced by nanoparticle Brownian motion.

For Al_2O_3 nanofluid at Re = 1000, h rises from 66.12 $W/m^2 \cdot K$ at 5 % to 219.38 $W/m^2 \cdot K$ at 20 %, corresponding to a 231 % improvement. Fe_3O_4 nanofluid exhibits a more pronounced enhancement, with hhh increasing from 73.49 $W/m^2 \cdot K$ to 306.95 $W/m^2 \cdot K$ (a 318 % improvement) over the same range. The higher thermal conductivity of Fe_3O_4 (80.4 W/m·K) compared to Al_2O_3 (40.0 W/m·K) accounts for its superior performance.

3.2 Effect Of Reynolds Number

Increasing Reynolds number (Re) promotes greater turbulence intensity in the tube-side flow, leading to thinning of the thermal boundary layer and higher convective heat transfer rates. For 10 % Al_2O_3 nanofluid, h increases from 81.72 $W/m^2 \cdot K$ at Re = 200 to 165.99 $W/m^2 \cdot K$ at Re = 1000, representing a 103 % improvement. Fe_3O_4 nanofluid at the same concentration shows an increase from 89.74 W/m²·K to 247.13 W/m²·K, corresponding to a 175 % gain.

These results confirm that both nanoparticle loading and flow velocity are synergistic in enhancing convective performance, with Fe_3O_4 delivering higher incremental gains at elevated Re. The combined influence of nanoparticle volume fraction and Reynolds number is visualized through temperature contour plots in Figs. 5 and 6. For low ϕ and Re (e.g., ϕ = 5 %, Re = 200), temperature gradients are shallow and the thermal boundary layer remains thick. As ϕ and Re increase, the contours become denser near tube walls, indicating stronger convective transport. Fe_3O_4 nanofluids exhibit more intense temperature gradients and reduced hot spots compared to Al_2O_3 under equivalent conditions, underscoring their higher thermal conductivity and stronger disturbance of the near-wall thermal layer.

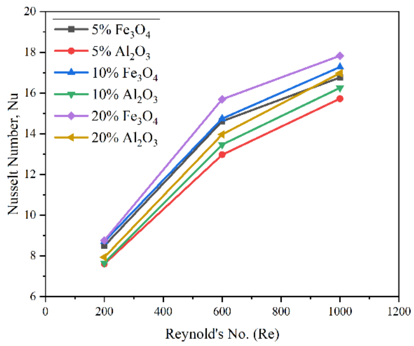

Fig.4. A comparative Nusselt number plot (Nu vs. Re)

(a) **(b)** **(c)**

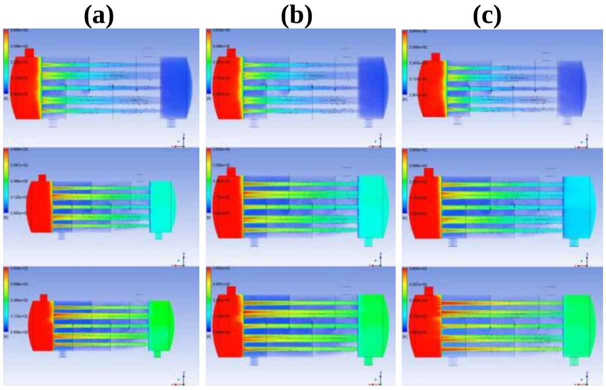

Fig. 4: *Temperature contours for Al_2O_3–water nanofluid at ϕ = 5 %, 10 %, and 20 % with Re = 200, 600, and 1000.*

(a) **(b)** **(c)**

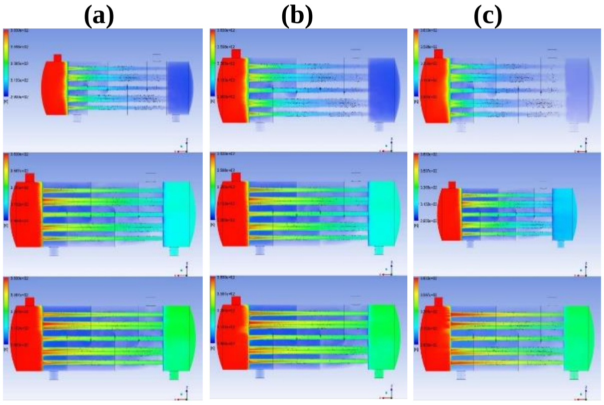

Fig. 5. Temperature contours for Fe_3O_4–water nanofluid at ϕ = 5 %, 10 %, and 20 % with Re = 200, 600, and 1000.

3.3 Temperature Variation

The thermal distribution of the nanofluids at the local scales was examined at three typical points of the heat exchanger namely, the centerline of the tube, the area around the walls, and the tube outlet. "Fig.6(a)-(b)" shows the results of Fe_3O_4-water and Al_2O_3 -water at 20% of the time. As anticipated, higher Reynolds number lowers the fluid temperature at any place as a result of greater convective transport. The temperature of the centerline also drops gradually with Re which means that the bulk heat removal is also improved. Fe_3O_4 always has low centerline temperatures relative to Al_2O_3 at the same flow rate, the difference being even more significant at high Re. Indicatively, at Re = 1000 centerline temperature of Fe_3O_4 is approximately 325 K compared to 332 K of Al_2O_3 which demonstrates the better cooling capacity of Fe_3O_4. The temperature profiles against the wall tend the same way. A nanofluid with Fe_3O_4 forms a thinner thermal boundary layer resulting in increased heat extraction on the wall and reduced wall temperature when compared to Al_2O_3. This is directly related to the increased Nusselt numbers which were experienced with Fe_3O_4. Lastly, Fe_3O_4 reaches much lower bulk fluid temperatures than Al_2O_3 at the outlet section. At Re = 1000, the temperature of the outlet is lowered to approximately 315 K of Fe_3O_4 and approximately 325 K of Al_2O_3. It means that under the same conditions of operation Fe_3O_4 will provide better overall cooling.

(a)

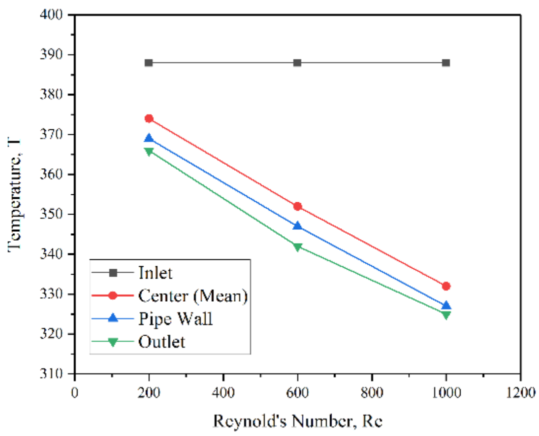

(b)

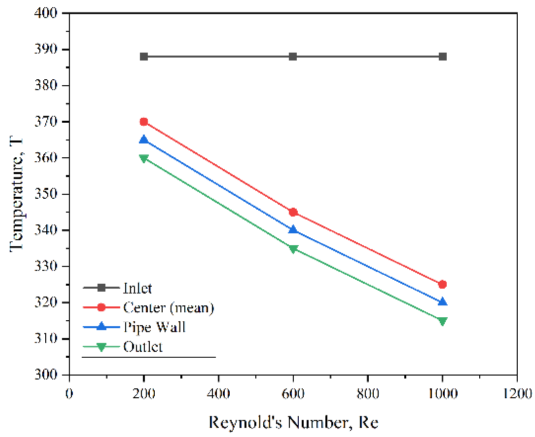

Fig. 6. Temperature variation at representative locations of the heat exchanger for (a) Fe_3O_4–water nanofluid and (b) Al_2O_3–water nanofluid at φ = 20%: centerline, near-wall, and outlet temperatures

3.4 Nusselt Number Trends

The variation of Nusselt number (Nu) with Reynolds number for different nanoparticle concentrations is shown in "Figs. 7 and 8". For all cases, Nu increases with both *Re* and ϕ, consistent with the trends observed for hhh in Sections 3.1–3.2. Fe_3O_4 nanofluid achieves the highest *Nu* values, with the maximum recorded at $\phi = 20$ % and *Re* = 1000.

The improvement in Nu is attributed to both the higher effective thermal conductivity and the increased convective transport from enhanced mixing in the fluid core. These results align with experimental findings by Gupta et al. [7] and Akhavan-Behabadi et al. [8]. The increasing Nusselt number with Reynolds number can be attributed to boundary layer thinning and enhanced mixing at higher velocities. Importantly, Fe_3O_4 exhibits a steeper slope compared to Al_2O_3, suggesting that nanoparticle thermal conductivity has a synergistic effect with flow inertia. These findings are consistent with Buongiorno's theory of convective transport in nanofluids [4]. The improvement is particularly significant at $\phi = 20\%$ and Re = 1000, where Nu for Fe_3O_4 is nearly 40% higher than that for Al_2O_3 under identical conditions.

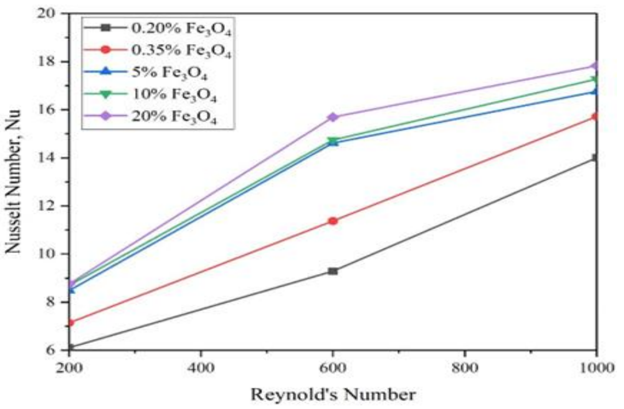

Fig. 7. Variation of Nusselt number with Reynolds number for Fe_3O_4–water nanofluid at different volume fractions.

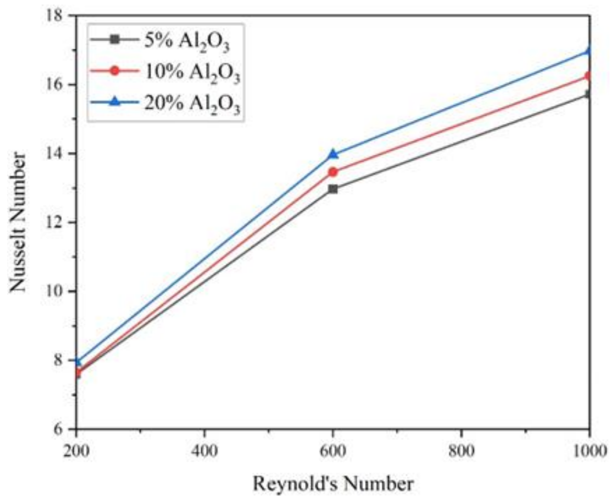

Fig. 8. Variation of Nusselt number with Reynolds number for Al_2O_3–water nanofluid at different volume fractions.

A comparative **Nu–Re plot ("Fig. 4")** shows that both nanofluids exhibit increasing Nusselt numbers with rising Reynolds number and concentration. Fe_3O_4 consistently outperforms Al_2O_3, achieving a maximum Nu ≈ 17.8 at Re = 1000 and $\phi = 20\%$. The widening performance gap at higher Re highlights Fe_3O_4's superior thermal conductivity and stronger convective enhancement.

"Figure 8" directly compares the performance of Al_2O_3 and Fe_3O_4 nanofluids. It is evident that Fe_3O_4 consistently achieves higher heat transfer coefficients across all Re and ϕ, attributable to its higher intrinsic thermal conductivity (80.4 W/m·K vs. 40.0 W/m·K for Al_2O_3). While both nanofluids show monotonic enhancement with Re, the relative gain of Fe_3O_4 is more pronounced at higher Reynolds numbers, indicating stronger coupling between nanoparticle thermal conductivity and flow-induced mixing.

4. Conclusions

A three-dimensional CFD analysis was conducted to compare Fe_3O_4-water and Al_2O_3-water nanofluids in a shell-and-tube heat exchanger under laminar conditions. The simulations confirmed that increasing nanoparticle concentration and Reynolds number substantially enhances the convective heat transfer coefficient and Nusselt number. Fe_3O_4 consistently outperformed Al_2O_3, achieving up to a 318% improvement in heat transfer and approximately 40% higher Nusselt numbers at equivalent conditions. The superior performance of Fe_3O_4 is attributed to its higher intrinsic thermal conductivity and stronger disturbance of the near-wall thermal boundary layer. Temperature contour and outlet profile analyses also revealed more uniform and lower fluid temperatures for Fe_3O_4, confirming improved cooling effectiveness. These findings suggest that Fe_3O_4 nanofluids offer significant promise for compact, high-efficiency heat exchangers in energy and process industries. However, considerations such as viscosity increase and potential pumping penalties at higher concentrations should be addressed. Future work should extend this investigation to turbulent flow, hybrid nanofluids, and experimental validation to further verify the practical feasibility of nanofluid-enhanced heat exchangers.

References

[1] R. K. Shah and D. P. Sekulic, *Fundamentals of heat exchanger Design*. John Wiley & Sons, 2003.

[2] Y. Xuan and Q. Li, "Heat transfer enhancement of nanofluids," *International Journal of Heat and Fluid Flow*, vol. 21, no. 1, pp. 58–64, Feb. 2000

[3] S. K. Das, S. U. S. Choi, and H. E. Patel, "Heat Transfer in Nanofluids—A review," *Heat Transfer Engineering*, vol. 27, no. 10, pp. 3–19, Sep. 2006

[4] J. Buongiorno, "Convective transport in nanofluids," *Journal of Heat Transfer*, vol. 128, no. 3, pp. 240–250, Aug. 2005

[5] S. M. Peyghambarzadeh, S. H. Hashemabadi, S. M. Hoseini, and M. S. Jamnani, "Experimental study of heat transfer enhancement using water/ethylene glycol based nanofluids as a new coolant for car radiators," *International Communications in Heat and Mass Transfer*, vol. 38, no. 9, pp. 1283–1290, Jul. 2011

[6] E. Manay and B. Sahin, "Heat transfer and pressure drop of nanofluids in a microchannel heat sink," *Heat Transfer Engineering*, vol. 38, no. 5, pp. 510–522, Jun. 2016

[7] L. S. Sundar, M. K. Singh, and A. C. M. Sousa, "Investigation of thermal conductivity and viscosity of Fe3O4 nanofluid for heat transfer applications,"

International Communications in Heat and Mass Transfer, vol. 44, pp. 7–14, Mar. 2013

[8] M. Attalla and H. M. Maghrabie, "An experimental study on heat transfer and fluid flow of rough plate heat exchanger using Al2O3/water nanofluid," *Experimental Heat Transfer*, vol. 33, no. 3, pp. 261–281, Jun. 2019

[9] S. Najim, A. Hussein, and S. H. Danook, "Performance improvement of shell and tube heat exchanger by using Fe3O4/water nanofluid," *Journal of Thermal Engineering*, vol. 9, no. 1, pp. 24–32, Jan. 2023

NOMENCLATURE

Symbol	Meaning	Unit
T	Temperature	K
P	Pressure	Pa
A	State transition matrix	Dimensionless
Cp	Specific heat capacity	J/kg·K
D_h	Hydraulic diameter	m
h	Convective heat transfer coefficient	W/m²·K
k	Thermal conductivity	W/m·K
μ	Dynamic viscosity	Pa·s
ϕ	Nanoparticle volume fraction	–
ρ	Density	kg/m³
Nu	Nusselt number (hD_h/k_{nf})	–
Re	Reynolds number ($\rho UD_h/\mu$)	–
U	Mean flow velocity	m/s